of this volume of the journal. Photocopies of the supplementary material from this paper only or microfiche (105 × 148 mm, 24× reduction, negatives) containing all of the supplementary material for the papers in this issue may be obtained from the Journals Department, American Chemical Society, 1155 16th St., N.W., Washington, D.C. 20036. Remit check or money order for $4.00 for photocopy or $2.50 for microfiche, referring to code number AIC403814.

References and Notes

(1) This work was performed under the auspices of the U.S. Atomic Energy Commission. The crystal structure was initially reported at the American Crystallographic Association Meeting, March 1974; see Abstract No. F2.
(2) L. H. Brooks, E. V. Garner, and E. Whitehead, "Chemical and X-Ray Crystallography Studies on Uranyl Fluoride," IGR-TN/CA 277, 1956.
(3) N. Bartlett and P. L. Robinson, *J. Chem. Soc.*, 3549 (1961).
(4) M. G. Otey and R. A. LeDoux, *J. Inorg. Nucl. Chem.*, **29**, 2249 (1967).
(5) R. T. Paine, *Inorg. Chem.*, **12**, 1457 (1973).
(6) R. T. Paine, R. S. McDowell, and L. B. Asprey, *Inorg. Chem.*, in press.
(7) P. W. Wilson, *J. Chem. Soc., Chem. Commun.*, 1241 (1972).
(8) E. Jacob and W. Polligkeit, *Z. Naturforsch. B*, **28**, 120 (1973).
(9) D. F. Shriver, "The Manipulation of Air Sensitive Compounds," McGraw-Hill, New York, N.Y., 1969; B. Weinstock, *Rec. Chem. Progr.*, **23**, 23 (1962).
(10) J. G. Surak, D. J. Fisher, C. L. Burros, and L. C. Bates, *Anal. Chem.*, **32**, 117 (1960).
(11) H. T. Evans, *Acta Crystallogr.*, **14**, 689 (1961).
(12) W. R. Busing and H. A. Levy, *Acta Crystallogr.*, **10**, 180 (1957).
(13) (a) R. R. Ryan and D. T. Cromer, *Inorg. Chem.*, **11**, 2322 (1972); (b) W. H. Zachariasen, *Acta Crystallogr.*, **23**, 558 (1967); (c) A. C. Larson, *ibid*, **23**, 664 (1967).
(14) A. C. Larson, unpublished Los Alamos Scientific Laboratory system of crystal structure programs.
(15) "International Tables for X-ray Crystallography," Vol. IV, Kynoch Press, Birmingham, England, in press.
(16) D. Cromer and D. Liberman, *J. Chem. Phys.*, **53**, 1891 (1970).
(17) Supplementary material.
(18) D. F. Smith, *Science*, **140**, 899 (1963).
(19) H. Selig, C. W. Williams, and G. J. Moody, *J. Phys. Chem.*, **71**, 2739 (1967).
(20) G. H. Dieke and A. B. F. Duncan, "Spectroscopic Properties of Uranium Compounds," McGraw-Hill, New York, N.Y., 1949, p 245.
(21) Unpublished room-temperature spectra from this laboratory.
(22) W. H. Beattie, unpublished work from this laboratory.
(23) M. J. Vasile and W. E. Falconer, private communication.
(24) H. R. Hockstra, *Inorg. Chem.*, **2**, 492 (1963).
(25) R. D. Peacock, *Advan. Fluorine Chem.*, **7** (1973), on structures of $MoOF_4$, WOF_4, $TcOF_4$, and $ReOF_4$.
(26) A. G. Robiette and K. Hedberg, private communication on WOF_4.
(27) L. E. Alexander, I. R. Beattie, A. Bukovsky, P. J. Jones, and C. J. Marsden, *J. Chem. Soc., Dalton Trans.*, 81 (1974), on $MoOF_4$ and WOF_4; P. Tsao, C. C. Cobb, and H. H. Claassen, *J. Chem. Phys.*, **54**, 5247 (1971), on $XeOF_4$.
(28) G. Gundersen and K. Hedberg, *J. Chem. Phys.*, **51**, 2500 (1969).
(29) (a) W. H. Zachariasen, *Acta Crystallogr.* **1**, 277 (1948); (b) M. Atoji and M. J. McDermott, *ibid.*, **26**, 1540 (1970).
(30) W. H. Zachariasen, *Acta Crystallogr.*, **7**, 783 (1954).
(31) A. Rosenzweig and R. R. Ryan, submitted for publication in *Amer. Mineral.*
(32) J. Laveissiere, *Bull. Soc. Fr. Mineral. Cristallogr.*, **90**, 308 (1967); R. A. Penneman, R. R. Ryan, and A. Rosenzweig, *Struct. Bonding (Berlin)*, **13**, 1 (1973).
(33) H. M. Seip, *Acta Chem. Scand.*, **19**, 1955 (1965).
(34) J. C. Taylor and P. W. Wilson, *J. Chem. Soc., Chem. Commun.*, 232 (1974).

Contribution No. 2176 from the Central Research Department, E. I. du Pont de Nemours and Company, Wilmington, Delaware 19898

Diffusionless Orthorhombic to Hexagonal Transitions in Ternary Silicides and Germanides

V. JOHNSON

Received October 22, 1974 AIC40727A

Stoichiometric MnCoGe and MnNiGe are orthorhombic, ordered Co_2P type at room temperature and not hexagonal Ni_2In type as previously reported. These germanides and the corresponding silicides transform diffusionlessly at elevated temperatures to the hexagonal Ni_2In structure. For the germanides, the orthorhombic to hexagonal transition temperature changes rapidly with small compositional changes. These transitions (*Pnma* to $P6_3/mmc$) like those between closely related MnP and NiAs structures are ferroelastic. The crystallographic, phase analytical, and magnetic properties of hexagonal and orthorhombic forms presented suggest the importance of metal–metal bonding to the relative stability of these structures.

Introduction

MnCoGe and MnNiGe were first reported[1] to have the hexagonal Ni_2In structure. Powder patterns of MnCoSi and MnNiSi[2,3] were indexed as orthorhombic, ordered Co_2P type.[4,5] (This orthorhombic structure is also described as anti-$PbCl_2$ or TiNiSi type. Here we use ordered Co_2P type to emphasize relationships with the MnP and "filled-NiAs" (Ni_2In) type.) Magnetic properties were reported[6] for the germanides. Only Austin[7] identified crystallographic transitions in compositions close to MnCoGe and MnNiGe.

Contrary to most reported results, we find all four phases, MnCoSi, MnNiSi, MnCoGe, and MnNiGe, to be isostructural at room temperature with the orthorhombic, ordered Co_2P-type structure if compositions are maintained close to equiatomic. They all transform to the hexagonal Ni_2In structure at elevated temperatures. We describe here preparation, crystallographic and magnetic properties, and some phase analytical results for compositions close to MnCoGe.

Experimental Section

Sample Preparation. MnCoSi and MnNiSi were prepared as described elsewhere.[8]

MnCoGe and MnNiGe were prepared from high-purity elements (99.999%) in Al_2O_3-lined silica tubes between 800 and 1050°. An Al_2O_3 liner is necessary to prevent reaction with the silica tube which drastically alters the nominal stoichiometry. In a typical reaction, 99.999% Mn (purified by partial sublimations), 99.999% Co powder (H_2 reduced), and intrinsic grade Ge in the atomic ratio 1:1:1 were sealed under vacuum in an Al_2O_3-lined silica tube, fired at 975° for 16 hr and slowly cooled. (The weight loss after this firing step was 0.086%, which, assuming only Mn losses, corresponds to the composition $Mn_{0.997}CoGe$.) The sample was then crushed, resealed in another Al_2O_3-lined silica tube, fired at 1050° for 2 hr, cooled to 700°, held for 16 hr, and cooled quickly. The resulting ingot shattered on cooling to room temperature. (The weight loss at this stage was 0.396%, which, again assuming only Mn losses and neglecting mechanical losses, corresponds to $Mn_{0.987}CoGe$.) Similar procedures were used for the preparation of other compositions close to MnCoGe and MnNiGe.

Structural Studies. Room-temperature *d* values were measured by the Hägg-Guinier X-ray powder diffraction technique. Cell dimensions were obtained by least-squares refinement.

Several high-temperature X-ray powder techniques were used to study the structural transformations. Powder diffractometry under dry helium in a Tempres camera and a GE diffractometer was used for MnCoSi. Patterns (Cr radiation) were recorded according to the following sequence: 25, 800, 900, 975, 900, 800, and 25°. In a second experiment, powder patterns of MnCoSi were obtained at 25 and

Table I. Cell Dimensions of Ternary Manganese Silicides and Germanides

Compn	Temp	Structure	*a*, Å	*b*, Å	*c*, Å	*V*/*Z*, Å^3
MnCoSi	Room	Orth Co_2P	5.8643 (5)	3.6872 (4)	6.8548 (5)	37.05
MnNiSi	Room	Orth Co_2P	5.8967 (6)	3.6124 (5)	6.9162 (6)	36.82
MnCoGe	Room	Orth Co_2P	5.9572 (8)	3.8168 (8)	7.0542 (11)	40.10
MnNiGe	Room	Orth Co_2P	6.0421 (6)	3.7550 (4)	7.0860 (6)	40.20
$Mn_{0.975}NiGe$	Room	Orth Co_2P	6.0268 (5)	3.7581 (4)	7.0714 (5)	40.05
MnCoSi	1000°	Hex Ni_2In	4.03		5.29	37.20
MnNiSi	1000°	Hex Ni_2In	4.04		5.38	38.02
MnCoGe	135°	Hex Ni_2In	4.10		5.36	39.01
$Mn_{0.975}CoGe$	Room	Hex Ni_2In	4.0835 (4)		5.3097 (5)	38.34
$Mn_{0.95}CoGe$	Room	Hex Ni_2In	4.067		5.300	37.96

Table II

Compn	T_t, °C	Compn	T_t, °C
MnCoSi	917	$Mn_{0.975}CoGe$	20
MnNiSi	933	MnNiGe	220
MnCoGe	125–185		

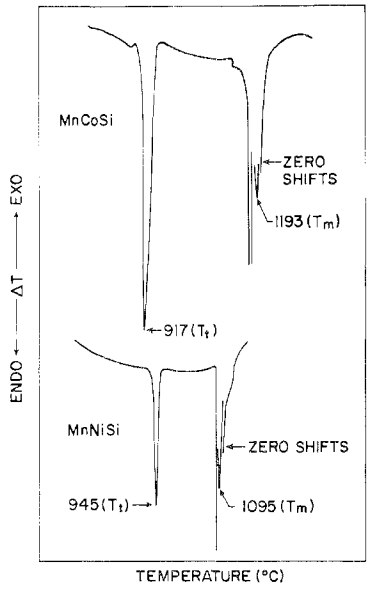

Figure 1. Dta traces of endothermic peaks for MnCoSi and MnNiSi. T_m is the melting point and T_t is the Co_2P to Ni_2In transition temperature on heating.

1000°. Impurity lines due to partial oxidation were present in the 1000° pattern, but these could be identified, allowing indexing of the high-temperature phase. MnNiGe was studied between 25 and 400° by the same technique. MnNiSi was studied at 800, 1000, and 800°, sequentially by the Debye–Scherrer technique (Unicam high-temperature camera) with Cu radiation. Patterns obtained were poor but permitted identification of the high-temperature phase and demonstrated the reversibility of the transition. MnCoGe was studied under helium between 25 and 160° with an MRC camera and a Norelco diffractometer, with Cu radiation.

Structural transitions were also studied by dta in the case of the silicides and by dsc for the germanides using a Du Pont 900 thermal analyzer. Measurements were done under argon. Magnetic properties of MnCoGe were determined with a vibrating-sample magnetometer.

Results

Table I lists the cell dimensions of all four phases. The Co_2P to Ni_2In crystallographic transition temperatures, T, are given in Table II. T_t is defined as the endothermic peak on heating (Figures 1 and 2). For the germanides, T_t is extremely sensitive to stoichiometry; $Mn_{0.95}CoGe$, for example, is hexagonal down to 4.2 K. This explains the large difference (125–185°) in T_t for different MnCoGe samples and also the fact that "MnCoGe" has been previously reported to be hexagonal Ni_2In type. For compositions $Mn_{1-x}Co_{1-y}Ge$, the orthorhombic structure was observed only at room temperature for $0 \leq x \leq 0.05$ at $y = 0$ and for $0 \leq y \leq 0.05$ at $x = 0$. Compositions outside this range (over a wide range of x and y as yet not precisely determined) are hexagonal Ni_2In type. T_t for MnNiGe varies somewhat more slowly with composition, while the silicides show no significant variation.

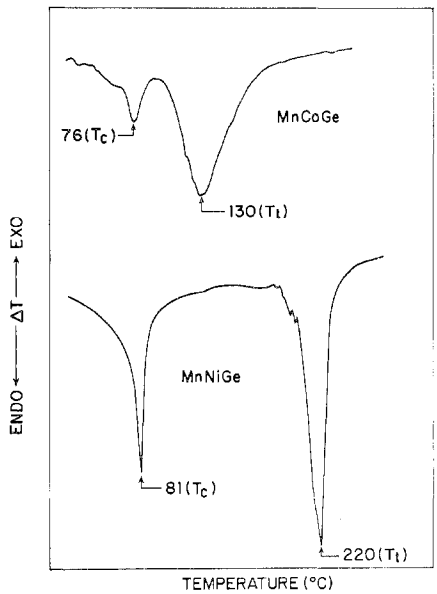

Figure 2. Dsc traces of endothermic peaks for MnCoGe and MnNiGe. T_c is the magnetic ordering temperature and T_t is the Co_2P to Ni_2In transition temperature on heating.

Table III. Room-Temperature Powder Pattern of Orthorhombic MnCoGe[a]

hkl	I_{obsd}	d_{obsd}	d_{calcd}
101	5	4.5514	4.5513
102	30	3.0361	3.0350
200	20	2.9807	2.9786
112	70	2.3761	2.3755
210	30	2.3505	2.3482
202	30	2.2756	2.2757
211	100	2.2283	2.2280
103	25	2.1866	2.1872
013	50	2.0023	2.0020
301	60	1.9108	1.9114
020			1.9084
113	40	1.8980	1.8977
004	5	1.7623	1.7635
121			1.7600
302	20	1.7304	1.7304
311	10	1.7086	1.7091
213	20	1.6617	1.6615
122	5	1.6155	1.6156
204	10	1.5176	1.5175
303			1.5171
400	2	1.4891	1.4893
222	10	1.4624	1.4623
123	5	1.4375	1.4380
105	10	1.3729	1.3728
402			1.3720
321	20	1.3516	1.3505

[a] Space group *Pnma*, $a = 5.9572$ (8) Å, $b = 3.8168$ (8) Å, $c = 7.0542$ (11) Å, and $V = 160.39$ (3) Å^3.

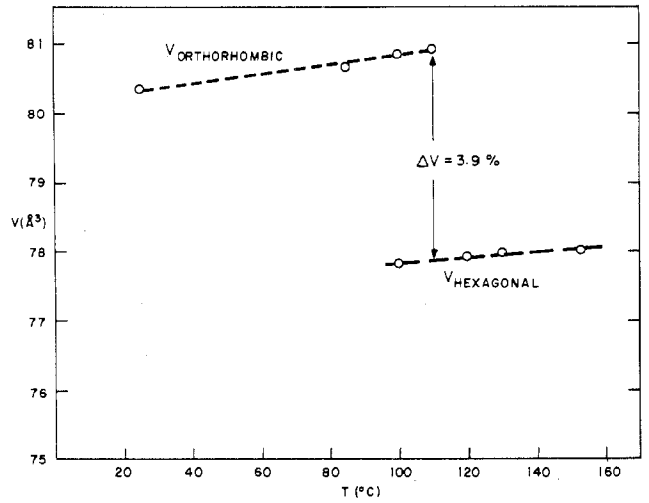

Figure 3. Cell volume *vs.* temperature for MnCoGe (T_t(from dsc) = 125°).

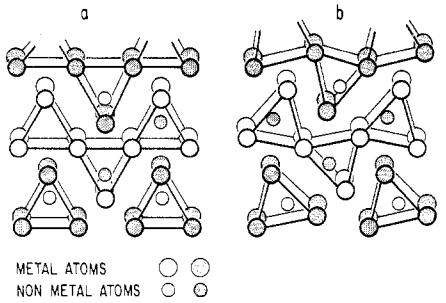

Figure 4. Relationship between (a) Ni_2In and (b) Co_2P structures.

Table IV. Magnetic Properties of Compositions Close to MnCoGe

Compn	Structure	T_c, °K	μ_S, μ_B/molecule
MnCoGe	Co_2P	355 (5)	3.86
$Mn_{0.975}CoGe$	Co_2P	300[a]	3.67
$Mn_{0.95}CoGe$	Ni_2In	265	2.58

[a] On heating, T_c coincides with T_t and hence shows hysteresis.

The powder pattern of a sample of MnCoGe (T_t = 180°) is given in Table III. The cell volume of another sample (T_t = 125°) is given as a function of temperature in Figure 3. The Co_2P to Ni_2In transition in this sample is accompanied by a large (~3.9%) negative volume change, which is responsible for the severe cracking of cast specimens on cooling. In fact, ~25% of one cast specimen could be reduced to <50-μ particle size by repeated cycling through T_t.

The transitions in all four phases are reversible and fast indicative of a diffusionless mechanism. They also exhibit large hysteresis and hence are first order.

Magnetic Properties. Magnetic properties of the silicides have been reported elsewhere.[8] MnCoGe, $Mn_{0.975}CoGe$, and $Mn_{0.95}CoGe$ are ferromagnetic. Curie temperatures and magnetic moments are listed in Table IV. We have not determined magnetic properties for MnNiGe.

Discussion

The relationship between the Co_2P and Ni_2In structures has been discussed by several authors.[9-11] Figure 4 shows that interdiffusion of ions is not required for the distortions that produce the Co_2P structure from Ni_2In. Diffusionless phase transitions are therefore readily understandable. Co_2P to Ni_2In transitions have also been observed for the binaries Ni_2Si and Co_2Si[12] and the ternaries TiNiSi and TiCoSi.[13] According to Aizu,[14] their space groups (hexagonal $P6_3/mmc$ for Ni_2In and orthorhombic *Pnma* for Co_2P) are connected by a ferroelastic transformation. Micrographs of cast Ni_2Si (Figure 5) show within individual crystallites twin boundaries or ferroelastic domain walls from the Co_2P to Ni_2In transition. Such walls are also observed in intermetallics which undergo martensitic transformations. NiAs-related phases which transform "martensitically" at low temperatures are usually brittle and tend to fracture along the domain walls, *e.g.*, MnAs.[17] Presumably, Ni_2Si is sufficiently ductile at T_t (>1200°) to deform plastically rather than fracture. The essential difference between the ferroelastic NiAs-related phases and the martensites which show the "memory" effect [*e.g.*, TiNi, Cu_3Al, etc.[18]] therefore appears to be the magnitude and mechanism of plastic deformation.

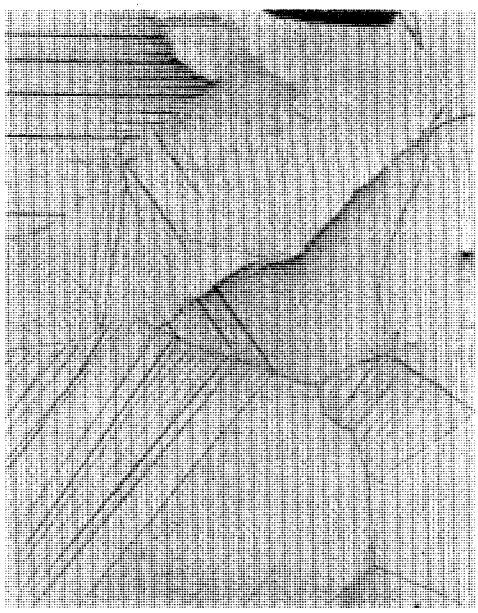

Figure 5. Micrograph of Ni_2Si prepared from the melt. Irregular lines are grain boundaries; straight lines are ferroelastic domain walls.

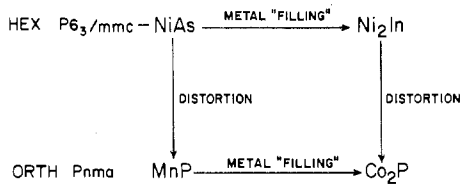

Figure 6. Relationships among NiAs, Ni_2In, MnP, and Co_2P structures.

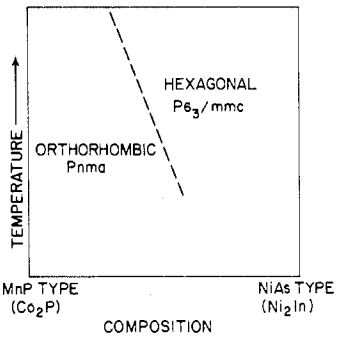

Figure 7. Schematic phase diagram for simple NiAs–MnP or Ni_2In–Co_2P systems.

The four structures NiAs, MnP, Ni_2In, and Co_2P types are closely related (Figure 6). Diffusionless transitions between MnP and NiAs forms have been observed in the CrAs–CrSb[15] and CrAs–CrSe[16] systems. The hexagonal NiAs and Ni_2In structures are high-temperature forms of the orthorhombic structures. (MnAs undergoes a transition from the NiAs structure to the MnP structure with increasing temperature;

Table V

	$Mn_{0.975}CoGe$	MnCoGe
$c_{hex} = a_{orth}$, Å	5.3097	5.952
$a_{hex} = b_{orth}$, Å	4.084	3.822
$\sqrt{3}a_{hex} = c_{orth}$, Å	7.073	7.050
V/Z, Å^3	38.34	40.10

here, however, the magnetic contribution to the free energy is responsible.) A generalized phase diagram for these orthorhombic and hexagonal phases is shown in Figure 7. Materials with transitions may be found in appropriate solid solutions between orthorhombic and hexagonal forms. Since these transitions are diffusionless, they can easily go undetected and, in many systems, may also be preceded by the melting point of the compound.

An interesting feature of the Co_2P–Ni_2In transition in MnCoGe is the large negative contraction at T_t (Figure 3). Unit cell axes of the two structures are related as

$$a_{orth} = c_{hex}$$

$$b_{orth} = a_{hex}$$

$$c_{orth} = \sqrt{3}a_{hex}$$

Another indication of how these axes change at the transition for MnCoGe may be obtained by comparing orthohexagonal axes of $Mn_{0.975}CoGe$ with those of MnCoGe at room temperature (Table V). Such a comparison does reflect the structural changes at the transition since the volumes of hexagonal $Mn_{0.975}CoGe$ and $Mn_{0.95}CoGe$ differ by <1%, but orthorhombic MnCoGe is larger than hexagonal $Mn_{0.975}CoGe$ by ~5%. Distortion of the high-symmetry cell occurs primarily in the orthohexagonal *ab* plane. Atomic displacements leading to the distortion in MnCoGe are discussed more fully elsewhere.[19]

We have previously mentioned[20] that the high-symmetry structures (NiAs and Ni_2In) are stable with respect to the distorted variants (MnP and Co_2P) in compounds with larger metalloids. This trend is evident in the compounds discussed here, since transition temperatures decrease in the order silicides > germanides > stannides. In fact, none of the first-row transition metal stannides have the Co_2P structure above room temperature. This suggests that metal–metal bonding *via* d orbitals contributes significantly to the binding energy in the orthorhombic forms. The narrower phase fields of the orthorhombic forms are also consistent with this speculation. Generally, the orthorhombic, low-temperature forms are "enthalpy stabilized" whereas the hexagonal high-temperature forms are "entropy stabilized." Goodenough[21] argued that in ternary phases, ordering of M and M' produces anisotropic elastic forces required for stabilization of the orthorhombic phase.

Magnetic Properties. Magnetic properties of compositions close to MnCoGe are extremely sensitive to the Mn concentration (Table IV). T_c decreases quite rapidly but linearly with Mn deficiency, and the magnetic moment decreases abruptly when the symmetry changes from orthorhombic to hexagonal.

We have argued previously that metal–metal bonding is primarily responsible for the greater stability of the orthorhombic phase. Stronger metal–metal bonding is expected in MnCoSi *vs.* MnCoGe since it has shorter M–M distances. The larger moment of MnCoGe (3.86 μ_B) *vs.* MnCoSi (~3.2 μ_B) is therefore consistent with this interpretation, which implies narrower d bands in MnCoGe. In these systems, Mn carries a much larger moment than Co or Ni.[8] The main differences in M–M bonding between orthorhombic and hexagonal structures is the closer Mn–Mn separations in the hexagonal phase and much closer Co–Co separations in the orthorhombic phase. The reduction in the moment of the hexagonal phase is therefore most likely due to wider Mn d bands in this phase.

Acknowledgment. The author is grateful to C. G. Frederick for magnetic measurements, H. Williams for dta and dsc measurements, G. A. Jones and W. Evans for high-temperature X-ray work, and J. Amalfitano for help with sample preparation.

Registry No. MnCoSi, 12526-44-2; MnNiSi, 12401-76-2; MnCoGe, 12516-07-3; MnNiGe, 54062-05-4.

References and Notes

(1) L. Castelliz, *Monatsh. Chem.*, **84**, 765 (1953).
(2) Yu. B. Kuz'ma and E. I. Gladyshevskii, *Russ. J. Inorg. Chem.*, **9**, 373 (1964).
(3) Yu. B. Kuz'ma, E. I. Gladyshevskii, and E. E. Cherkashin, *Russ. J. Inorg. Chem.*, **9**, 1028 (1964).
(4) C. B. Shoemaker and D. P. Shoemaker, *Acta Crystallogr.*, **18**, 900 (1965).
(5) W. Jeitschko, A. G. Jordan, and P. A. Beck, *Trans. AIME*, **245**, 335 (1969).
(6) L. Castelliz, *Z. Metallk.*, **46**, 198 (1955).
(7) A. E. Austin, Battelle Memorial Institute, private communication.
(8) V. Johnson and C. G. Frederick, *Phys. Status Solidi, A*, **20**, 331 (1973).
(9) F. Jellinek, *Z. Österr. Chem.*, **60**, 311 (1959).
(10) B. Aronsson, T. Lundstrom, and S. Rundqvist, "Silicides, Borides, and Phosphides," Methuen and Co., London, 1965, p 69.
(11) V. Johnson and W. Jeitschko, *J. Solid State Chem.*, **4**, 123 (1972).
(12) *Izv. Akad. Nauk SSSR, Neorg. Mater.*, **8**, 3468 (1972).
(13) V. Johnson, unpublished work.
(14) K. Aizu, *J. Phys. Soc. Jap.*, **27**, 387, (1969).
(15) A. Kallel and H. Boller, *Solid State Commun.*, **12**, 665 (1973).
(16) V. Johnson, to be submitted for publication.
(17) Z. S. Basinski, R. O. Kornelsen, and W. B. Pearson, *Trans. Indian Inst. Metals*, **13**, 141 (1960).
(18) A. Nagasawa, *J. Phys. Soc. Jap.*, **31**, 136 (1971).
(19) W. Jeitschko, to be submitted for publication.
(20) V. Johnson, *Mater. Res. Bull.*, **8**, 1067 (1973).
(21) J. B. Goodenough, *J. Solid State Chem.*, **7**, 428 (1973).